

Tb³⁺-Yb³⁺ cooperative down and up conversion processes in Tb_{0.81}Ca_{0.19}F_{2.81}:Yb³⁺ single crystals

P. Molina,^{1,a)} V. Vasyliiev,^{1,2} E. G. Vllora,¹ and K. Shimamura¹

¹National Institute for Materials Science, 1-1 Namiki, Tsukuba 305-0044, Japan

²Waseda University, Graduate School of Advanced Science and Engineering, Department of Nanoscience and Nanoengineering, 3-4-1 Okubo, Shinjuku-ku, Tokyo 169-8555, Japan

(Received 12 September 2011; accepted 15 November 2011; published online 29 December 2011)

The energy transfer processes between Tb³⁺ and Yb³⁺ ions are studied in Tb-based fluoride single crystals. These are very transparent from the UV to the IR wavelength regions, except for the characteristic absorption lines of the rare-earth ions under study. In contrast with previously reported Tb³⁺-doped glasses and oxide powders, these crystals containing a high Tb³⁺ concentration present two major advantages for the study of the energy transfer processes in the Tb³⁺-Yb³⁺ ion pair. Firstly, the adverse influence of host defects is minimized with the use of high quality crystals. Secondly, the high Tb³⁺ concentration guarantees a much higher absorption cross-section of UV light, and consequently these crystals have real potential for practical applications. Photoluminescence spectra in the visible-IR wavelength region demonstrate the existence of efficient down and up conversion processes by crossed excitation and emission characteristics of Tb³⁺ and Yb³⁺ ions. In the down conversion process, Tb³⁺(⁵D₄) → 2Yb³⁺(²F_{5/2}), two IR photons are emitted for each Tb³⁺ ion deexcited by second-order energy transfer to two Yb³⁺ ions. The total quantum efficiency of the down conversion process in the fluoride system is shown to increase linearly with the Yb³⁺ concentration, reaching its maximum at the Yb³⁺ solubility limit in the fluoride host. Further, efficient up conversion by two- and three-IR photon absorption is observed. © 2011 American Institute of Physics. [doi:10.1063/1.3671406]

I. INTRODUCTION

Down conversion (DC) processes are used in different applications to increase the light yield of luminescent materials. DC consists in the absorption of a high energy photon and the subsequent emission of two or more photons of lower energy, such that the quantum efficiency (QE) can be over 100% and the thermalization losses can be minimized. Multiphoton DC emission was proposed by Dexter in the mid-1950s,¹ and nowadays, taking advantage of the excellent luminescence properties of rare earth (RE³⁺) ions, DC efficiencies close to 200% have been claimed.^{2,3} Due to its potential applications in mercury-free fluorescence tubes and plasmas displays, the DC mechanism has been widely investigated in different systems that transform deep UV light into visible light.⁴⁻⁶

More recently, UV-visible converters have been proposed to increase the efficiency of standard Si-solar cells.⁷⁻⁹ In this particular case, the ideal DC system possesses a high absorption in the UV range (above double the Si band gap, i.e., 2E_{g,Si}), a high transparency in the visible range (between 2E_{g,Si} and E_{g,Si}), and a high DC QE in the IR range, emitting at an energy slightly greater than E_{g,Si}. Among the different DC mechanisms involving RE³⁺ ions, those based on the energy transfer (ET) between an ion pair have been found to be more efficient and more flexible for better matching the required energy scheme. At present, the Tb³⁺-Yb³⁺ pair is the most promising one. In this particular case, an UV

photon absorbed by Tb³⁺ above the ⁵D₄ → ⁷F₆ transition at λ = 485 nm (~2E_{g,Si}) leads via an ET process to the Yb³⁺ emission of two IR photons, corresponding to the ²F_{5/2} → ²F_{7/2} transition at λ = 980 nm (above E_{g,Si} at λ = 1100 nm).

Due to the absence of overlap between Tb³⁺ and Yb³⁺ electronic levels, this Tb³⁺ → Yb³⁺ ET process is recognized as a cooperative second-order one.³ Although these kinds of ET processes in general show lower efficiencies than first-order ones, in the particular case of Tb³⁺-Yb³⁺, QEs higher than 100% have been reported in several systems such as KYb(WO₄)₂:Tb³⁺,¹⁰ Tb³⁺-Yb³⁺ codoped silica glass,¹¹ (Yb,Y)PO₄:Tb³⁺,³ and (Yb,Gd)Al₃(BO₃)₄:Tb³⁺.¹² At this point it is important to remark that all the previous reports based on oxide glasses and sintered powders consider the Tb³⁺ ion only like a dopant. This low concentration, together with the forbidden nature of the 4f-4f involved transitions, clearly limits the absorption cross section of Tb³⁺ in the UV/blue region. Consequently, even though ET QEs in Tb³⁺ → Yb³⁺ ions have been reported to be very high, this weak absorption dramatically limits the total external efficiency of the DC systems.

With this study we have aimed at the analysis of the Tb³⁺-Yb³⁺ DC process in a fluoride matrix having a high Tb³⁺ concentration as constituent. In contrast to oxides, fluorides are generally characterized by a large band gap and low phonon energies, which guarantee a larger transparency and higher radiative emission efficiencies, respectively. As a starting compound, Tb_{0.81}Ca_{0.19}F_{2.81} (TCF) was chosen. This melts congruently at 1222 °C,¹³ and high quality crystals can be grown by the Czochralski (Cz) technique under the proper atmosphere. It has been proposed for Faraday isolator

^{a)}Author to whom correspondence should be addressed. Electronic mail: molina.pablo@nims.go.jp.

applications in the visible range due to its high transmittance in this region and its high Tb^{3+} concentration.¹⁴ These properties, together with the possibility of incorporating large amounts of Yb^{3+} by isovalent substitution, make of this crystal an ideal system to further investigate the $\text{Tb}^{3+} \rightarrow \text{Yb}^{3+}$ DC. At this point it should be mentioned that the use of high quality single crystals has advantages in comparison with glasses and powders. By this it is possible to minimize the adverse effects of crystal defects on the ET in the Tb^{3+} - Yb^{3+} ion pair under study.

In the present work, we demonstrate the efficient DC process taking place in $\text{TCF}:\text{Yb}^{3+}$. In order to get a deeper understanding of the ET process in this system, both static and time-resolved luminescence measurements have been carried out on high quality single crystals. Further, the role played by the opposite process, namely, the $\text{Yb}^{3+} \rightarrow \text{Tb}^{3+}$ up conversion (UC), is also investigated and discussed.

II. EXPERIMENTAL

Highly transparent pure and Yb^{3+} doped TCF single crystals were grown by the Cz technique with a 30 kW RF generator. High purity raw materials (>99.99%) of commercially available CaF_2 , TbF_3 , and YbF_3 powders were weighted and mixed in a Pt-crucible. Taking the TCF congruent composition as a base, i.e., $\text{Tb}_{0.81(1-x)}\text{Yb}_{0.81x}\text{Ca}_{0.19}\text{F}_{2.81}$, different nominal Yb^{3+} concentration ratios relative to Tb^{3+} , ($N_{\text{Yb}} = \text{Yb}/(\text{Tb} + \text{Yb})$), were chosen: 2.5, 4, 5, 7.5, 10, and 15 mol %. The growth was carried out under CF_4 atmosphere (>99.99%) in order to avoid any contamination by oxygen. The rotation and the pulling rates were fixed at 10 rpm and 1 mm/h, respectively.

The chemical composition of grown crystals was determined via total reflection x-ray fluorescence using a TXRF 8030c FEI instrument. Due to the difference in ionic radius between Tb^{3+} and Yb^{3+} , a N_{Yb} gradient along the growth direction of the $\text{TCF}:\text{Yb}^{3+}$ crystals was observed, indicating that the Yb^{3+} segregation coefficient was below one in this system. For the sake of clarity, to each crystal a single N_{Yb} has been assigned, corresponding to a location close to that of the sample area used for the photoluminescence measurements. The N_{Yb} in the measured samples was found to be 2.4, 2.5, 3.8, 5.2, 8.4, and 10.9 mol %.

X-ray powder diffraction (XRD) patterns were recorded with a Rigaku XRD/RINT Ultima III diffractometer equipped with CuK_α radiation ($\lambda = 1.5418 \text{ \AA}$). The $\Theta/2\Theta$ scans were performed between $20^\circ < 2\Theta < 120^\circ$ with a step of 0.01° and a scan rate of $0.7^\circ/\text{min}$. The obtained patterns were analyzed with the software FULLPROF.¹⁵

Transmission spectra were measured with a PerkinElmer Lambda 900 spectrometer in the UV-near IR region. Photoluminescence was collected in perpendicular geometry and focused with a lens (10 cm focus) into a 0.5 m Spex monochromator. As excitation sources, a cw Ar^+ laser at 488 nm, a pulsed (10-30 Hz) N_2 gas laser at 337 nm, a tunable pulsed (10 Hz) optical parametric oscillator Spectra Physics Quanta-Ray 730 MOPO, and a Ti:sapphire Mira Optima 900-P Coherent operated in cw were used. The photoluminescence was detected with a Peltier-cooled charge coupled

device camera and a R5108 photomultiplier from Hamamatsu. The Yb^{3+} concentration quenching by auto-absorption was analyzed by means of an optical fiber coupled to a StellarNet spectrometer. The optical fiber was placed on a polished crystal surface while the excitation beam was continuously displaced to enhance the optical path. The lifetime measurements were carried out with the R5108 photomultiplier and with the aid of a Lecroy WaveRunner 6300 digital oscilloscope.

All the measurements were performed at room temperature.

III. RESULTS AND DISCUSSION

TCF melts congruently at 1222°C and crystallizes in the hexagonal system with space group $\text{P6}_3/\text{mmc}$, i.e., uniaxial with a tysonite structure.¹⁶ Fig. 1(a) shows a picture of a crack-free highly transparent $\text{TCF}:\text{Yb}^{3+}$ single crystal wafer grown by the Cz technique with $N_{\text{Yb}} = 3.8 \text{ mol \%}$ as an example. The photographs of cut and polished prisms under crossed polarizers are shown in Fig. 1(b) with different orientations. The absence of twin and stress features is indicative of the high optical quality of these crystals, and correspondence between the c - and optical axis is verified. The single crystalline nature of the $\text{TCF}:\text{Yb}^{3+}$ crystals has been confirmed by XRD measurements. Figure 2 shows the very good agreement between the measured XRD pattern and the calculated fit of the 3.8 mol % N_{Yb} sample. Similar results were obtained for the other crystals. The absence of additional peaks indicates that there is no secondary phase

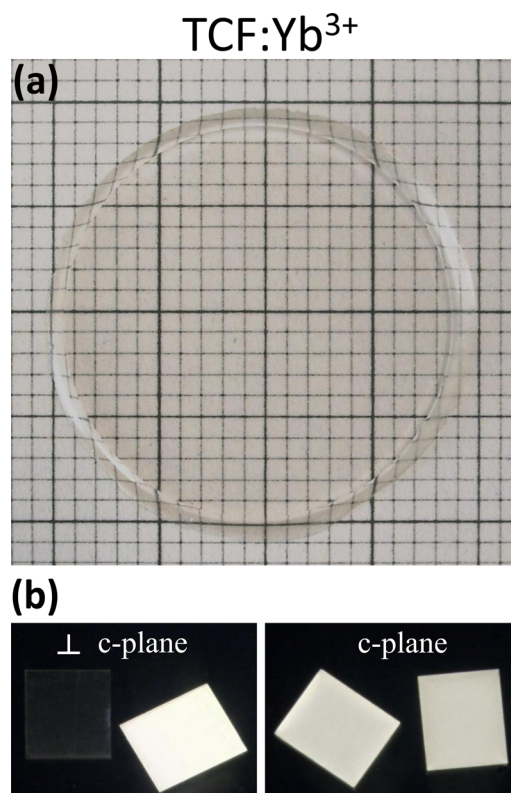


FIG. 1. (Color online) Photograph of (a) an as-grown $\text{TCF}:\text{Yb}^{3+}$ single crystal wafer of 3.8 mol % and (b) cut and polished oriented prisms under crossed polarizers.

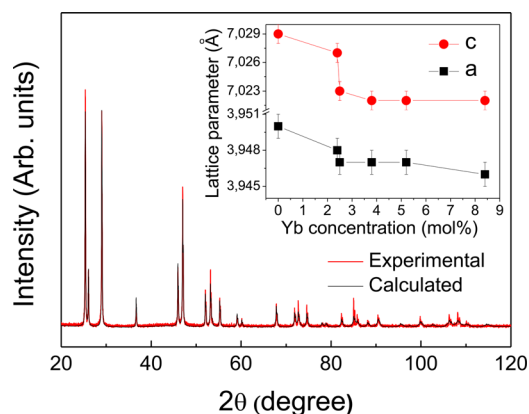


FIG. 2. (Color online) XRD pattern of 3.8 mol % TCF:Yb³⁺ together with the calculated fit.

segregation and that, as expected, the three cations are randomly distributed in the single cationic site. Yb³⁺ is incorporated in the crystal by the isovalent substitution of Tb³⁺. The growth of high quality single crystals was not possible for nominal values of N_{Yb} higher than 15 mol %. As can be seen in the inset of Fig. 2, and in accordance with the smaller ionic radii of Yb³⁺ respect to Tb³⁺, the a and c lattice parameters become smaller with the N_{Yb} up to a certain concentration. This suggests that the incorporation of Yb³⁺ is reaching a solubility limit, above which the structure is unstable. Therefore, crystals with higher concentrations were fully cracked after growth and consequently were disregarded for the following analysis.

The transparency range of TCF extends from 250 nm to 10 μ m, exhibiting in the visible range values over 90% without antireflection coating.¹⁴ This crystal is characterized by the Tb³⁺ absorption peaks around 250–385 nm (UV) and 488 nm (blue), which correspond to electronic transitions between the energy levels $^7F_6 \rightarrow ^5D_J$ for $J=2, 3$, and 4, respectively. As mentioned in the Introduction, these correspond to 4f–4f parity and spin forbidden transitions, so that the remarkable absorption intensity originates simply from the high Tb³⁺ concentration in this matrix. After the partial substitution of Tb³⁺, the concentration of Yb³⁺ in the samples can be inferred from the intensity of the broadband Yb³⁺ absorption peak centered around 975 nm, corresponding with the $^2F_{7/2} \rightarrow ^2F_{5/2}$ electronic transition. These facts are clearly illustrated in Fig. 3, where the transmittance of nominal 3.8 and 8.4 mol % TCF:Yb³⁺ single crystals is shown in comparison.

In order to investigate the ET process in the series of TCF:Yb³⁺ single crystals, emission spectra were recorded after excitation in the UV and blue regions, at 337 and 488 nm, respectively. The observed features of the luminescence spectra were independent of N_{Yb} and excitation wavelength; therefore, for the sake of clarity, only the results of 3.8 mol % are presented in detail.

Figure 4 shows the emission spectrum of this crystal upon 337 nm excitation in the Tb³⁺ $^7F_6 \rightarrow ^5D_2$ absorption band. After a fast non-radiative decay from the 5D_2 level, the first excited Tb³⁺ 5D_4 level is populated, from where a radiative recombination takes place. As a result, intense emission lines in the visible part of the spectrum peaking at

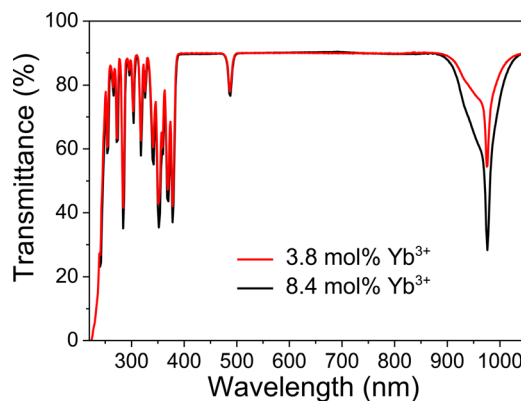


FIG. 3. (Color online) Transmittance spectra of 3.8 and 8.4 mol % TCF:Yb³⁺ single crystals in comparison.

488, 542, 585, 619, 652, 667, and 678 nm, and associated with the Tb³⁺ $^5D_4 \rightarrow ^7F_J$ ($J=6, 5, 4, 3, 2, 1$, and 0, respectively) electronic transition, are observed. In addition to the emission in the visible range, Fig. 4 shows a broadband emission in the near IR region centered at 975 nm. After confirming that we are avoiding the presence of second harmonics of Tb³⁺ $^5D_4 \rightarrow ^7F_J$ emissions via the use of appropriated filters, this emission at 975 nm is assigned to the electronic transition $^2F_{5/2} \rightarrow ^2F_{7/2}$ of the Yb³⁺ ion. This near IR emission exhibits a large linewidth broadening. This is characteristic for the Yb³⁺ ion and has been related to the intense electron-phonon coupling experienced by this ion. Taking into account the energy level diagram for Tb³⁺–Yb³⁺ ions, which allows only second-order ET DC processes between these ions, and the absence of additional ET paths in this host, in contrast to other materials,¹⁷ the observation of this Yb³⁺ emission band in the near IR region evidences that the Tb³⁺ \rightarrow Yb³⁺ ET DC is taking place in the TCF:Yb³⁺ system.

It is noteworthy in Fig. 4 that the TCF crystals do not present any emission from the 5D_3 electronic levels to the ground state ($^5D_3 \rightarrow ^7F_J$). Previous studies on compounds with Tb³⁺ as a constituent have shown that the quenching of this emission band with an increase in the Tb³⁺ concentration correlates with the enhancement of the emission band from the 5D_4 levels, indicating a non-radiative decay ($^5D_3 \rightarrow ^5D_4$) between both excited states.^{18,19} In an analogous manner,

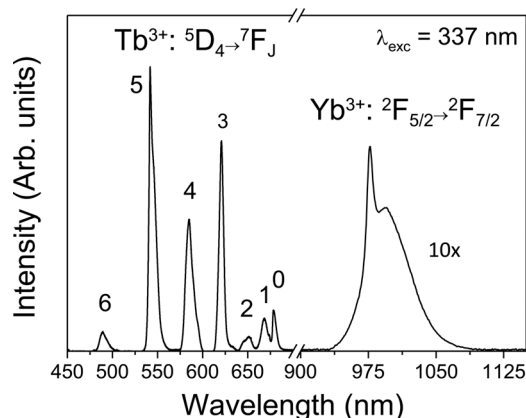


FIG. 4. Emission spectrum after UV excitation at 337 nm for 3.8 mol % TCF:Yb³⁺ single crystal.

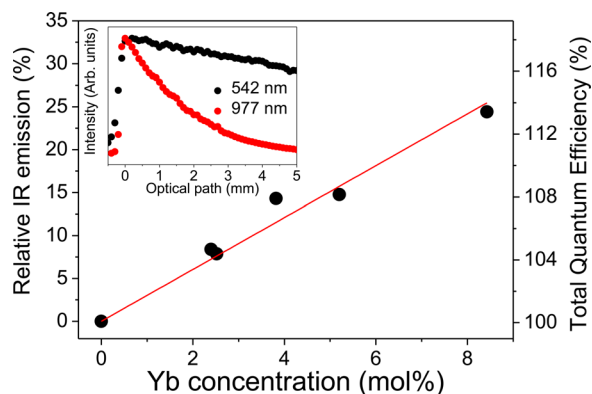


FIG. 5. (Color online) Relative IR emission efficiency and total QE as a function of N_{Yb} in TCF:Yb³⁺ single crystals. The inset shows the luminescence intensity as a function of the optical path for an absorbing (977 nm) wavelength and a non-absorbing (542 nm) one.

the absence of the $^5D_3 \rightarrow ^7F_5$ emission band in our TCF crystals is assumed to be caused by the high Tb³⁺ concentration.

Once the occurrence of the Tb³⁺ \rightarrow Yb³⁺ ET has been proved (Fig. 4), the process is analyzed. The relative intensity of the IR Yb³⁺ emission, i.e., $I_{IR}/I_{visible+IR}$, is shown as a function of the N_{Yb} in Fig. 5 (left ordinate). It is seen that the Yb³⁺ emission increases approximately linearly with the N_{Yb} , with a calculated proportionality factor of 2.8. Given that the Yb³⁺ emission can only occur in pairs by the second-order ET DC process, and that the Tb³⁺ concentrations are relatively high, we deduce the following: (a) Yb³⁺ ions are not distributed purely randomly, i.e., “far” from each other, but rather gather, for example, in pairs, as suggested by other authors. This is based on the fact that DC ET can occur only between neighboring Yb³⁺-Tb³⁺-Yb³⁺ ions. (b) Each Yb³⁺ pair receives the ET of more than one surrounding Tb³⁺ ion. These considerations can explain the relatively high IR Yb³⁺ emissions, with values well above the N_{Yb} , i.e., a high transfer efficiency.

At this point it should also be noted that special care has been taken to minimize IR auto-absorption losses, which occur with increasing N_{Yb} . For this, the excitation of the single crystals was done almost at the edge of the crystal close to the detector side. To estimate the possible errors occurring from Yb³⁺ concentration quenching, the intensity of the total IR emission was measured as a function of the distance for two wavelengths, as is shown in the inset of Fig. 5 for the sample with 3.8 mol % N_{Yb} . At 542 nm, the sample is transparent, and the decrease indicates basically that the emission collected by the optical fiber is decreasing as the solid angle becomes smaller with the distance. With the same configuration, but exciting at 977 nm, at the maximum overlap of direct Yb³⁺ excitation and emission spectra, the intensity shows an exponential decay. This indicates that Yb³⁺ auto-absorption will play an important role when the IR emission goes through thick samples. From these results we concluded that the emission intensities obtained close to the crystal edge are negligibly affected by Yb³⁺ auto-absorption or concentration quenching.

Assuming that the radiative emission efficiencies of the Tb³⁺ 5D_4 and Yb³⁺ $^2F_{5/2}$ excited states are one, which is generally accepted as a good approximation to the reality,

the total QE of the TCF:Yb³⁺ system has been evaluated as $I_{visible+IR}/I_{visible+IR/2}$. Due to the correspondence with Fig. 5, this is shown on the right ordinate. The proportionality factor is now 1.6, indicating that our system presents QEs well over the ones reported in the literature for similar N_{Yb} ,³ where the QEs are well below the N_{Yb} . In principle, this observed trend can last only for sufficiently low N_{Yb} , as long as the Yb³⁺ pairs are completely surrounded by Tb³⁺ ions. In fact, we have already observed a decreasing tendency for a sample of higher concentration, 10.9 mol % N_{Yb} (not shown). Even though several growth trials were undertaken, the obtained crystals were always fully cracked. Therefore, in order to avoid undesired crystal defects that would affect the intrinsic characteristic of the ET under study, these crystals with a deficient crystalline quality have been disregarded.

In order to get deeper insight into the characteristics of the TCF:Yb³⁺ system, fluorescence lifetime measurements have been carried out. Figure 6 shows the time-resolved luminescence of the Tb³⁺ $^5D_4 \rightarrow ^7F_5$ emission at 542 nm under pulsed excitation at 337 nm. All the crystals exhibit a non-single exponential decay, the lifetime of which depends on the N_{Yb} . The slowest decay is found for the pure TCF sample, with a lifetime of 3.21 ms (experimentally estimated at the intensity of I/e). In general, the initial deviation from the single exponential is attributed to a fast non-radiative energy migration between Tb³⁺ ions, which in our system is favored by the high Tb³⁺ concentration. With the partial substitution of Tb³⁺ by Yb³⁺, the decay time decreases, indicating the appearance of additional relaxation paths for the Tb³⁺ 5D_4 excited state. In the literature, for this Tb³⁺-Yb³⁺ pair, the lifetime decreases continuously with the N_{Yb} , and the only path considered has been the ET DC process. This could be reasonable for such systems due to the low Tb³⁺ content, which is just introduced as a dopant. In our case, however, a minimum lifetime is obtained for 3.8% N_{Yb} . The possible cause of this relative minimum is discussed in the next figure, where UC processes taking place in the system are evaluated. According to the standard analysis of experimental decay curves done by other authors in the Tb³⁺-Yb³⁺ system, the ratio between the integrated luminescence decay

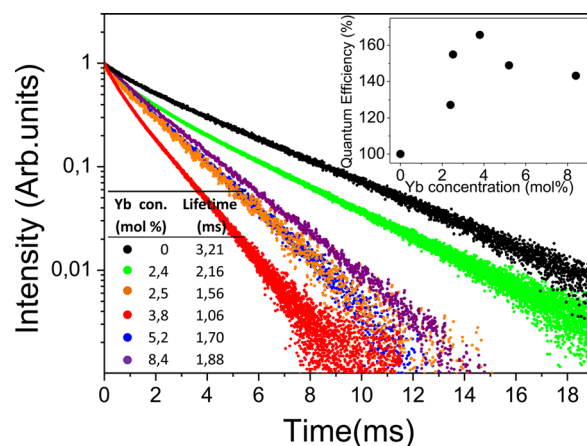


FIG. 6. (Color online) Time resolved luminescence of the Tb³⁺ $^5D_4 \rightarrow ^7F_5$ channel (emission at 542 nm) after excitation at 337 nm for the TCF:Yb³⁺ crystal family. The inset shows the QE, estimated from the total luminescence of the decay curves, as a function of the N_{Yb} .

curves of pure and Yb^{3+} doped samples is a measure of the efficiency of the ET process ($\text{QE}_{\text{ET-Yb}} = 1 - I_{\text{Yb}}/I_{\text{pure}}$).³ Here it is considered that all Yb^{3+} ions deexcite radiatively. Further, assuming that the $\text{Tb}^{3+} {}^5\text{D}_4$ QE is also one, an upper limit of the total QE of the system can be calculated ($\text{QE}_{\text{Total}} = 1 + \text{QE}_{\text{ET-Yb}}$). The results of this analysis are shown in the inset of Fig. 6. Here we can see that a relative maximum of the QE_{Total} as high as 165% is expected at 3.8 mol % N_{Yb} , and that the QEs are well above the ones determined experimentally by direct luminescent measurements in the visible and IR regions (see Fig. 5). This discrepancy indicates that the assumptions made for the evaluation of the decay curves are overestimates. Previous authors also found that their samples showed a much lower IR Yb^{3+} emission than the one estimated by the analysis of the decay curves, and they related this mismatch to the occurrence of Yb^{3+} concentration quenching. This argument cannot be applied to our system because, as mentioned in the discussion of Fig. 5, these losses have been minimized in our experimental setup. In our case, even though the adverse effects of auto-absorption and quenching on crystal defects have been minimized, there is still a remaining quenching that could explain the difference between the estimated total QEs deduced from $\text{Tb}^{3+} {}^5\text{D}_4$ decay times and the ones derived from the direct emission spectra.

Beyond the ET DC process, the second pathway considered in our TCF:Yb³⁺ system is the opposite one, the UC process by which two excited Yb^{3+} ions relax non-radiatively via the excitation of a neighboring Tb^{3+} ion into the ${}^5\text{D}_4$ state. This process has been proposed as a cooperative sensitization one by Salley *et al.*²⁰ Further, taking into account that Tb^{3+} is a constituent in this matrix, it is reasonable to presume that this process can play a relevant role in our system. The evidence of this UC process is given in Fig. 7 for the case of 8.4 mol % N_{Yb} , where the visible Tb^{3+} emission after the excitation in the Yb^{3+} absorption band at 920 nm is shown. All the crystals exhibit the UC process, and as can be expected, the intensity of the visible emission shows an increasing tendency with N_{Yb} . The emission intensity as a function of the pumping power is shown in the inset of Fig. 7. It is seen that the emission intensity increases by a

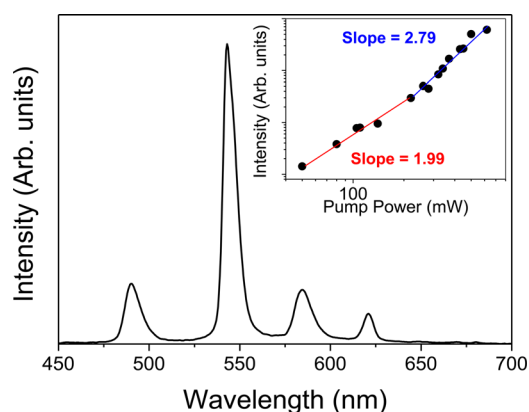


FIG. 7. (Color online) UC emission of $\text{Tb}^{3+} {}^5\text{D}_4 \rightarrow {}^7\text{F}_j$ after 920 nm excitation in the Yb^{3+} absorption band in TCF:Yb³⁺ with 8.4 mol % N_{Yb} . The inset displays the corresponding power dependence of the UC, indicating the occurrence of two and three IR photon absorption processes.

factor of close to 2 for pumping powers below 200 mW, whereas for higher powers this factor increases to almost 3. The first value is indicative of an UC process involving the absorption of two IR photons to populate the $\text{Tb}^{3+} {}^5\text{D}_4$ first excited state, whereas the second suggests a mixture of two- and three-photon absorption processes, with the latter being predominant.²¹ In this case the $\text{Tb}^{3+} {}^5\text{D}_2$ excited state is populated and relaxes non-radiatively to the ${}^5\text{D}_4$ level, from which the radiative visible emission takes place.

So far, it has been demonstrated that the studied TCF:Yb³⁺ system undergoes simultaneous DC and UC processes at the Tb^{3+} -Yb³⁺ pair. It has been observed that for the high Tb^{3+} concentrations considered, both show an increasing tendency with N_{Yb} . It should be noted, however, that their effect on the $\text{Tb}^{3+} {}^5\text{D}_4$ decay time is the opposite. The ET DC process, which is a very rapid radiative pathway, favors a faster depopulation of the $\text{Tb}^{3+} {}^5\text{D}_4$ level, and therefore it decreases the lifetime. In contrast, the UC process could repopulate the original $\text{Tb}^{3+} {}^5\text{D}_4$ level and consequently promote an increase in the lifetime.

In our crystals, the UC can be comparatively efficient due to the good matching of the energy levels of both ions and to their high concentrations as compound constituents. However, the UC following a DC process presumably has a low efficiency, and therefore the influence of the UC on the lifetime variation may be disregarded in a first approximation. Instead, we consider that the observed increase in the $\text{Tb}^{3+} {}^5\text{D}_4$ lifetime for N_{Yb} higher than 3.8 mol % might be associated with the appearance of lattice defects, as mentioned in the context of Fig. 2.

The presented TCF:Yb³⁺ system shows the practical limitations of the combination of Tb^{3+} and Yb^{3+} as a pair for DC processes. Previous works have been done on Tb^{3+} -Yb³⁺ codoped oxide powders synthesized via solid state reaction. The crystalline quality of these powders is very low in comparison with single crystals, and consequently their optical characterization involves all kinds of crystal and grain boundary defects. Further, as Tb^{3+} is incorporated only as a dopant, the external absorption is very low. Consequently, even under the assumption of very high ET QE (favored by a very high $\text{Yb}^{3+}/\text{Tb}^{3+}$ ratio), the external efficiency is correspondingly very low. In contrast to previous works, our single crystals of high crystalline quality allow us to get a clear picture of the Tb^{3+} -Yb³⁺ pair. The choice of a host with Tb^{3+} as a constituent is fundamentally important, because from a practical point of view this determines the amount of external light that the system can absorb for the DC process (see Fig. 3). This facilitates the isovalent substitution of both RE ions, Tb^{3+} and Yb^{3+} . This is essentially important for finding a proper balance between the basically relevant optical processes involved in the system as a total, namely, the total absorption, the ET QE, and the Yb^{3+} concentration quenching. In our TCF:Yb³⁺ system we have seen that for the N_{Yb} considered, the total QE is limited only by the crystalline quality, which dramatically diminishes for N_{Yb} over approximately 8.4 mol %. Therefore, in order to explore the limits of the Tb^{3+} -Yb³⁺ pair, it would be necessary to use another host that can guarantee a higher $\text{Yb}^{3+}/\text{Tb}^{3+}$ ratio while maintaining the high crystalline quality.

IV. CONCLUSIONS

The present work has focused on the first study of Tb^{3+} - Yb^{3+} ET DC in single crystals. The host utilized, TCF, contains Tb^{3+} as a constituent, and through isovalent RE substitution crystals with different Yb^{3+} concentrations have been successfully grown via the Cz technique. In contrast to previous studies, based on Tb^{3+} - Yb^{3+} codoped oxide powders, we have investigated a system that efficiently absorbs the external light. Consequently, the external efficiency of the Tb^{3+} - Yb^{3+} pair is remarkably improved. Efficient DC by second-order ET involving $\text{Tb}^{3+}({}^5\text{D}_4) \rightarrow 2\text{Yb}^{3+}({}^2\text{F}_{5/2})$ ions is demonstrated by photoluminescence measurements. It is shown that the total radiative QE increases linearly with the N_{Yb} up to a maximum of 114% for 8.4 mol % N_{Yb} . The optimum concentration ratio for the Tb-Yb pair could not be reached due to the solubility limit of Yb^{3+} in TCF. In addition to the DC process, the opposite process—the efficient first-order UC process—is demonstrated in the same Tb^{3+} - Yb^{3+} pair. Depending on the pumping power, the UC involves the absorption of two or three IR photons to repopulate the $\text{Tb}^{3+}({}^5\text{D}_4)$ first excited state.

ACKNOWLEDGMENTS

This work has been partially supported by the Ministry of Education, Science, Sports and Culture, Grant-in-Aid for Scientific Research (C), 22560316, 2010. The authors are

grateful to Professor L.E. Bausá and Dr. M.O. Ramírez for helpful discussions and measurements.

- ¹D. L. Dexter, *Phys. Rev.* **1**, 630 (1957).
- ²R. T. Wegh, H. Donker, K. D. Oskam, and A. Meijerink, *Science* **283**, 663 (1999).
- ³P. Vergeer, T. J. H. Vlugt, M. H. F. Kox, M. I. den Hertog, J. P. J. M. van der Eerden, and A. Meijerink, *Phys. Rev. B* **71**, 014119 (2005).
- ⁴C. R. Ronda, T. Justel, and H. Nikol, *J. Alloys Compd.* **277**, 669 (1998).
- ⁵C. Feldmann, T. Justel, C. R. Ronda, and P. J. Schmidt, *Adv. Funct. Mater.* **13**, 511 (2003).
- ⁶Q. Y. Zhang and X. Y. Huang, *Prog. Mater. Sci.* **55**, 353 (2010).
- ⁷T. Trupke, M. A. Green, and P. Würfel, *J. Appl. Phys.* **92**, 1668 (2002).
- ⁸B. S. Richards, *Sol. Energy Mater. Sol. Cells* **90**, 2329 (2006).
- ⁹B. S. Richards, *Sol. Energy Mater. Sol. Cells* **90**, 1189 (2006).
- ¹⁰W. Strek, A. Bednarkiewicz, and P. J. Deren, *J. Lumin.* **92**, 229 (2001).
- ¹¹I. R. Martin, A. C. Yanes, J. Mendez-Ramos, M. E. Torres, and V. D. Rodríguez, *J. Appl. Phys.* **89**, 2520 (2001).
- ¹²Q. Y. Zhang, C. H. Yang, and Y. X. Pan, *Appl. Phys. Lett.* **90**, 021107 (2007).
- ¹³B. P. Sobolev and P. P. Fedorov, *J. Less-Common Met.* **60**, 33 (1978).
- ¹⁴V. Vasyliiev, P. Molina, E. G. Villora, and K. Shimamura, *Opt. Mater.* **33**, 1710 (2011).
- ¹⁵J. Rodríguezcarvajal, *Physica B* **192**, 55 (1993).
- ¹⁶L. P. Otroschenko, B. P. Alexandrov, B. A. Maximov, V. I. Simonov, and B. P. Sobolev, *Kristallografiya* **30**, 658 (1985).
- ¹⁷J. L. Yuan, X. Y. Zeng, J. T. Zhao, Z. J. Zhang, H. H. Chen, and X. X. Yang, *J. Phys. D* **41**, 105406 (2008).
- ¹⁸L. G. Vanuiter and L. F. Johnson, *J. Chem. Phys.* **44**, 3514 (1966).
- ¹⁹E. J. Popovici, M. Nazarov, L. Muresan, D. Y. Noh, L. B. Tudoran, E. Bica, and E. Indrea, *J. of Alloys and Compd* **497**, 201 (2010).
- ²⁰G. M. Salley, R. Valiente, and H. U. Gudel, *J. Lumin.* **94**, 305 (2001).
- ²¹F. W. Ostermay and L. G. Vanuiter, *Phys. Rev. B* **1**, 4208 (1970).